High-Performance Mn-Al-O Catalyst on Reticulated Foam Materials for Environmentally Friendly Catalytic Combustion

S.A. Yashnik[1], V.V. Ushakov[1], N.L. Leonov[2], Z.R. Ismagilov[1,3*]

[1]Boreskov Institute of Catalysis SB RAS, pr. Akad. Lavrenteva, 5, Novosibirsk, Russia
[2]Institute of powder metallurgy NASB, Platonov Srt. 41, Minsk, Belarus
[3]Institute of Coal Chemistry and Materials Science SB RAS, pr. Sovetskiy 18, Kemerovo, Russia

Abstract

MnO_x supported on alumina and La_2O_3-modified alumina have been prepared and characterized as methane combustion catalysts. X-ray diffraction (XRD) analysis has revealed the significant low-temperature interaction between MnO_x and alumina, resulting in a solid solution $Mn-La-\gamma^*-Al_2O_3$ and a hexaaluminate formation upon thermal treatment at 900-1000 ºC and 1300 ºC, respectively. Mn-Al-O and Mn-La-Al-O catalysts washcoated on highly porous reticulated foam materials (RFM) have been prepared by two methods, such as: 1) a wet impregnation of a washcoating alumina layer on RFM by Mn and La nitrate solutions, 2) a dip coating of RFM into Mn-La-Al-containing suspension. The chemical compositions of RFM were cordierite, Ni, and NiCr-alloy. The catalytic activity of washcoated RFM in the methane combustion has been compared with one of granulated catalysts. The influence of alumina form ($\gamma-Al_2O_3$, $(\gamma+\chi)-Al_2O_3$, $\alpha-Al_2O_3$), manganese loading (5 and 10 wt.%), modifying agent (La_2O_3) on catalytic activity have been studied. Catalytic performances of Mn-Al-O and Mn-La-Al-O catalysts washcoated on RFM and pretreated in methane-containing atmosphere at 1100 ºC have been investigated. The Mn-Al-O catalyst modified by La_2O_3 and supported on RFM have been tested in a prototype catalytic water heating boiler and demonstrated a considerable reduction in the emissions of NO_x and CO compared to the conventional household boilers. The washcoating of the Mn-La-Al-O catalyst over surface of RFM provides a substantial reduction of toxic emissions during the catalytic fuel combustion. While an optimal foam structure and composition of the RFM provide improved heat and mass transfer properties of the catalyst in fuel combustion.

1. Introduction

Flameless catalytic combustion is a promising method for the increase of combustion efficiency and abatement of toxic emissions [1, 2]. In this process, the reactions of fuel oxidation proceed on the catalyst surface at low temperatures (300-750 ºC), providing total fuel conversion to the products of deep oxidation and preventing the formation of nitrogen oxides. One of the most interesting potential applications of the catalytic combustion is in the natural gas fuelled burners for production of heat energy, for example, in water-heating boiler, power-producing gas turbine plant [3]. Catalytic oxidation of carbon monoxide and hydrocarbon is also employed in catalytic converter of diesel engines [4-7].

In spite of the advantages of catalytic combustion, the key problem is to upgrade the known catalysts, in particular, to increase their catalytic activity and thermal stability to 1300 ºC. Noble metal catalysts (Pt, Pd) supported on alumina, cordierite, and metallic monolith with alumina washcoat are widely used in catalytic combustion and oxidation processes [6, 7]. Though Pt-catalysts exhibit high activity in the oxidation of hydrocarbons [8-10], they can not be used in the high-temperature combustion of fuels because Pt forms high-volatile compounds, such as PtO_2, at temperatures above 700 ºC [8, 9]. Palladium is less volatile than platinum [7], but cannot stand temperatures higher than 800 ºC because at 750-800 ºC PdO changes to metal Pd, which has much lower catalytic activity than that of PdO [10].

For increase of lifetime of the high-temperature catalyst, noble metal loading are increased to 3-5 wt.%, as result the cost of catalytic combustion chamber is increasing significantly [3].

Thermally stable catalysts based on metal oxides such as perovskites [8, 11, 12] and hexaaluminates [8, 13-16] are very attractive for the processes of high-temperature hydrocarbon fuel combustion. High thermal stability of hexaaluminates is determined by their crystal structure known as β-Al_2O_3 or magnetoplumbite [17]. The catalytic systems based on bulk [18] or supported [16, 19-22] manganese oxides are very promising for high-temperature combustion of hydrocarbon fuels, because of their high thermal stability up to 800-1000 ºC [18, 20] and to their ability to be activated at 900-1000 ºC [18, 21, 22].

In this work we continued synthesis and study of the oxide catalysts supported on highly porous reticulated foam materials (RFM, Fig.1A) based on ceramics and Ni-Cr alloy [23, 24]. The technology of preparation of the materials with a three-dimensional reticulated foam structure (ceramic and metal) is well-developed. The ceramic foam is prepared by duplicating the open-cellular polyurethane foam structure using suspensions on the basis of mixed ceramic powders (alumina, kaolin, talc, feldspar, pegmatite etc.) [25, 26]. The Ni-Cr alloy foam is prepared by duplicating the structure of open-cellular polyurethane foam using the suspension-electrochemical method and the subsequent thermal destruction agglomeration of the organic component [26]. The variation of initial powder compositions and high temperature synthesis conditions allows one to prepare ceramic foam with high mechanical strength, heat resistance and chemical durability. The main advantages of RFM are their high mechanical strength and heat conductivity permitting their application at high space velocities and heating to 1000-1100 ºC. Moreover, the internal structure of RFM allows minimizing the pressure drops, which is very important in some applications of catalytic combustion, such as catalytic boilers, heat exchanger, diesel exhaust gas convector, and other. Structural and frame properties of the ceramic and metal foams, provides favorable conditions for heat and mass transfer and high rate of external diffusion catalytic processes in ceramic and metal foams. The principal disadvantage of a as prepared RFM is low specific surface area.

To develop the specific surface area of RFM, alumina washcoat is deposited on the surface by different methods, such as dip coating in suspension, electrochemical deposition. This step is most difficult in the preparation of high-temperature catalysts. Because of weak adhesion of the washcoat to the metal support and different thermal expansion coefficients, the washcoat with a supported active component is flaking off and flown with a gas mixture during catalyst operation at high temperatures and high space velocities. Besides, highly developed surface area of γ-Al_2O_3, which is usually used as the main component of the washcoat [5, 16], tends to loose its high surface area under severe operating conditions. The critical loss of γ-Al_2O_3 surface area occurs above 1000 ºC with the transition to α-Al_2O_3 [27]. The stabilized additives, among which La_2O_3 being the most effective, allow a sintering processes to be inhibited [28].

The goal of the present work was to develop thermally stable manganese-alumina catalyst washcoated on RFM and to study their operation in the methane oxidation. We have investigated the catalytic properties in methane combustion of manganese-containing catalysts supported on pure and La-modified alumina washcoat in order to combine high activity at low temperature (related to the higher surface area) with wider range of thermal stability. Catalytic performances of Mn-Al-O catalysts washcoated on RFM and pretreated in methane-containing atmosphere at 1000-1100 ºC have been also investigated. Washcoating materials have been characterized by different physico-chemical methods in order to assess the influence of the modified agent on the catalytic features in methane combustion and thermal stability. We give example of RFM application in high-temperature combustion of hydrocarbon fuels as a part of the catalytic water-heating boiler and heat-exchanger.

2. Experimental

2.1. Preparation of granular Mn-Al-O catalysts

To optimize the composition of the Mn-Al-O washcoat, we have synthesized catalysts based on the granulated alumina. The alumina of different phase compositions: γ-Al_2O_3, (γ-+χ)-Al_2O_3, α-Al_2O_3, was prepared by hydrocarbon-ammonia formation. **Support 1** containing γ-Al_2O_3 was prepared using the commercial hydroxide with a pseudo-boehmite structure. **Support 2** containing γ-Al_2O_3 and 15% χ-Al_2O_3 was prepared from pseudo-boehmite resulting from thermal decomposition of gibbsite in the catalytic heat generator. The supports 1 and 2 were calcined at temperature 550 ºC. To prepare α-Al_2O_3 (**Support 3**), the γ-Al_2O_3 was calcined at 1200 ºC for 4 h.

The alumina supports were modified by incipient wetness impregnation with an aqueous solution of

lanthanum nitrate with following drying at 110 ºC and calcination at 550 ºC in air for 4 h. The lanthanum content was 5 wt.% calculated for La_2O_3. The physicochemical properties of the alumina supports were described in [28].

The Mn-Al-O catalysts were prepared by impregnating the support with an aqueous solution of manganese nitrate. Then the samples were dried at 110 ºC, calcined at 500 ºC in air flow for 4 h. A further calcination was performed at 900, 1100, and 1300 ºC for 4 h. The manganese loading in the catalysts was ~5 and ~10 wt.% calculated for MnO_2.

To investigate thermal stability, the catalysts were calcined at 1100 ºC for 20 h.

2.2. Preparation of washcoated catalysts based on RFM

In order to prepare washcoated catalysts, we used the highly porous reticulated foam material based on ceramics, Ni, and Ni-Cr alloy. They were produced by Institute of powder metallurgy (Minsk).

Foam-supported Mn-catalysts were prepared by two methods.

Method 1 was a wet impregnation of a alumina washcoating layer. It includes the below steps:

- preparation of a suspension, which contains 80% of powder of pure or La_2O_3-modified γ-Al_2O_3, (γ-+χ)-Al_2O_3 or α-Al_2O_3 and 20% of binder based on aluminum hydroxide with a pseudoboehmite structure as in ref. [20];

- washcoating of RFM with pure and La_2O_3-modified γ-Al_2O_3, (γ-+χ)-Al_2O_3, α-Al_2O_3 by its submerging into the suspension, drying and heating at 550 ºC for 4 h;

- wet impregnation of washcoated RFM with a manganese nitrate solution, drying and heating at 900 ºC for 4 h.

Method 2 was a direct deposition of Mn-Al-containing washcoat onto foam materials. It includes the below steps:

- preparation of the Mn-Al-powder by wetness impregnation of pure and La_2O_3-modified γ-Al_2O_3, (γ-+χ)-Al_2O_3, α-Al_2O_3 with a manganese nitrate solution, subsequent drying at 110 ºC, calcination at 500 ºC and grinding;

- preparation of a Mn-containing suspension by mixing the Mn-Al-powder (80%) and pseudoboehmite as a binder (20% calculated for Al_2O_3);

- deposition of the Mn-Al-containing washcoat onto RMF by dip coating, drying at 110 ºC and calcination at 900 ºC.

In both cases the manganese oxide loading in the washcoating layer was 5 and 10 wt.% calculated for MnO_2, lanthanum oxide loading was 5 wt.% calculated for La_2O_3. The washcoat content was 15-20 wt.%.

2.3. Catalyst characterization

The concentrations of Mn and La oxides were determined by atomic absorption spectroscopy with inductively coupled plasma (AAS – ICP) using a BLYRD analyzer.

XRD analysis was performed with a HZG-4 diffractometer using the Cu K$_\alpha$ radiation at $2\theta = 10$-70° at 1°/min. The JCPDS data file was used to identify the observed phases [29].

The textural properties of Mn-Al-catalysts was studied by adsorption method by measuring and processing the low-temperature (77 K) nitrogen adsorption isotherms using a volumetric automatic sorption installation ASAP-2400.

The SEM study was performed using a JSM 6460LV (JEOL, Japan) microscope with accelerating voltage 25 kV.

A thermocycling was used for study of washcoat layer adhesion strength. The sample was dried up to constant mass and weighed (M_0). Then it was heated to 900 ºC and fast cooled in water to 25 ºC. After that the sample was dried and weighed (M_n). The mass loss (ML) of the coating during thermocycling was calculated as:

$$ML = (M_0 - M_n) / M_0$$

where n is a thermocycling number.

Catalytic activity of Mn-Al-oxides supported on the RMF was studied in the reaction of methane oxidation using a flow reactor in the temperature range 200-700 ºC at a space velocity 1000 h^{-1}, the methane concentration in the initial gas mixture was 1 vol.% in air. The catalyst activity was characterized by temperature for 50% methane conversion ($T_{50\%}$). The reactants and reaction products were analyzed using a gas chromatograph equipped with a thermal conduction detector. A Porapak Q column (i.d. = 3 mm, L = 3 m) was used to separate the reaction products (CO, CO_2, CH_4). A molecular sieve 5A column (i.d. = 3 mm, L = 2 m) was used to determine the oxygen concentration.

3. Results and Discussion

3.1. Durability and heat resistance of reticulated foam materials based on Ni and Ni-Cr Alloy

During exploitation, the catalysts for high-temperature combustion are subjected to a complex of physic-chemical effects, beginning with high temperature and finishing with great aggressiveness of the reaction medium components due to the presence of sulfur containing compounds and formation of large amount of water vapor. Therefore the com-

bustion catalyst must possess high thermal stability and corrosion resistance. These properties are determined as a rule by the support properties.

Previously, using a number of instrumental methods, it was shown [26] that an increase of mechanical strength and heat resistance of reticulated foam materials based on nickel and nichrome was attained by the creation of connections between the layered structure with the outer layer of α-Al_2O_3 and Cr_2O_3, and inner layers of nickel aluminides with a varying composition (Fig. 1b).

The layer made from α-Al_2O_3 and Cr_2O_3 provides high heat resistance of materials in oxidative medium at 900 ºC [26]. In addition, the Cr_2O_3 layer ensures high durability of the material in oxidative sulfur containing media. For instance, heat resistance of Ni-18Cr-2Al reticulated foam material in oxidative sulfur containing atmosphere is practically 20-25 times higher in comparison with Ni based materials, including diffusion-aluminized ones [26].

A variable composition of heat resistant nickel aluminides from the δ-Ni_2Al_3 layer to the γ-phase (solid solution of Al in Ni) provides a gradual change of the thermal expansion coefficient, which decreases thermal tension during exploitation [26]. The plastic middle of the connection from the γ-phase promotes an increase of fatigue durability of the support, although the Ni_xAl layers have increased brittleness. Compressive strengths of diffusion-aluminized materials based on Ni-Al and Ni-18Cr-2Al are different by a factor of two and are equal to 4.6 MPa and 2.2–2.4 MPa, respectively [26].

In this work, we studied the influence of the chemical composition of the framework of reticulated foam materials and the effect of the presence of diffusion α-Al_2O_3 layer on their resistance to oxidation in air at 800, 1000 and 1200 ºC. The main physico-chemical characteristics of the foam materials – initial and calcined at high temperatures are given in Table 1. It can be seen that in all cases a growth of the calcination temperature from 600 to 1200 ºC leads to an increase of the content of oxide phase in the support observed both by the weight gain of the samples after calcination and by XRD data (Fig. 2). The formation of diffusion-aluminized layer of α-Al_2O_3 on structured Ni-supports results in a substantial increase of the resistance to oxidation at temperatures above 800 ºC. Gravimetric data show that the aluminization of Ni materials allows a decrease of the NiO phase content by ~3 times at all studied temperatures (Table 1), although, according to XRD, the formation of some amounts of NiO and α-Al_2O_3 phases takes place. The aluminization of structured Ni-Cr based materials has less effect on the resistance to oxidation in comparison with Ni materials. This can be explained by the formation of

the sub-layer of Ni_xAl intermetallides during aluminization of Ni based materials. These intermetallides have higher resistance to oxidation than Ni-Al and Ni-Al-Cr solid solutions. At a rise of the calcination temperature an increase of specific surface area is observed, more apparent in case of structured Ni materials. However the calcination at temperatures above 1000 ºC in oxidative medium results in cracking of diffusion aluminized layer of α-Al_2O_3 (Fig. 3a and b) and can further lead to the oxidation of the framework of the structured material with formation of NiO (Fig. 2b).
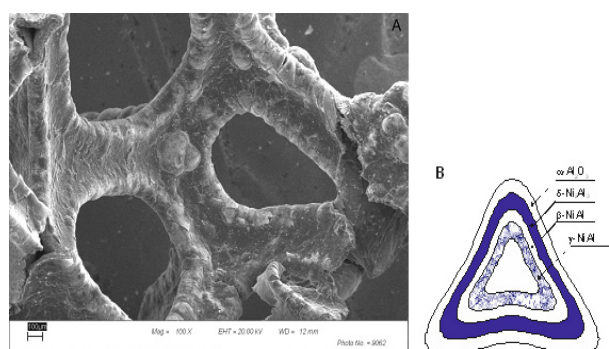

Fig. 1. External view (a) and schematic representation of layers (b) of Ni reticulated foam materials with diffusion layer of α-Al_2O_3 supported by diffusion aluminization.
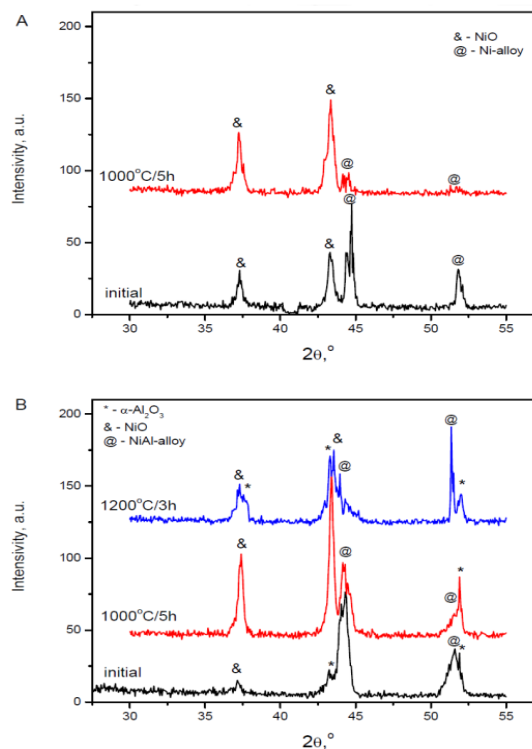

Fig. 2. Diffraction patterns of the reticulated foam materials based on Ni (a) and Ni with diffusion layer of α-Al_2O_3 supported by diffusion aluminization (b) before and after calcination at 1000 and 1200 ºC.
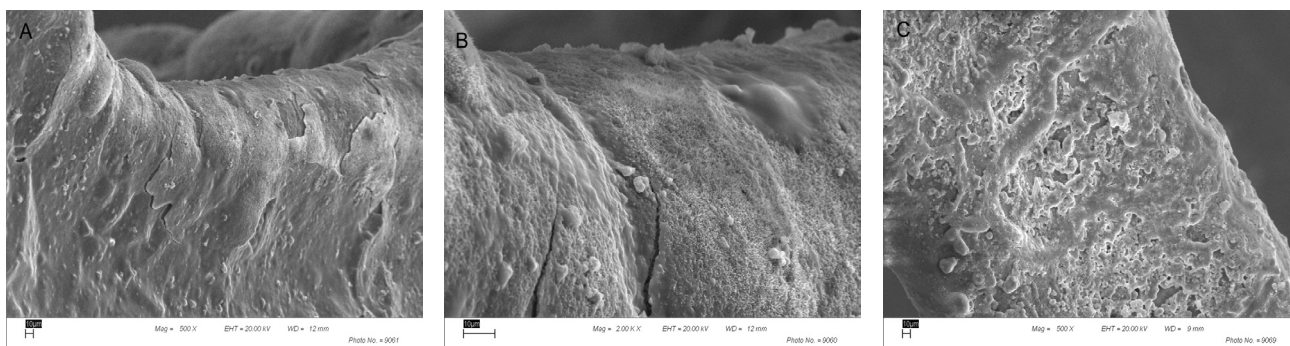
Fig. 3. SEM images of Ni RFM with diffusion layer of α-Al$_2$O$_3$ supported by diffusion aluminization (a), it after calcination at 1200 ºC in air (b), it after deposition of α-Al$_2$O$_3$ supported by dip coating (c).

Table 1

Physico-chemical properties of reticulated foam materials calcined in air at 800, 1000 and 1200 ºC for 20 h

#.	RFM chemical composition	Temperature pretreatment in air, ºC	Over-weight, %	XRD-phase composition	Specific surface area, m^2/g
1.	Ni	600	0	Ni	< 0.1
		800	1.2	Ni, NiO (trace)	~ 0.3
		1000	6.5	Ni, NiO	~0.5
		1200	20	Ni, NiO (main)	~0.5
2.	Ni-Al (alumunizing)	600	0	NiAl-alloy, α-Al$_2$O$_3$ and NiO (trace)	<0.1
		800	0.5	NiAl-alloy, α-Al$_2$O$_3$ and NiO	<0.1
		1000	2	NiAl-alloy, α-Al$_2$O$_3$ and NiO	~0.1
		1200	7.5	NiAl-alloy, α-Al$_2$O$_3$ and NiO*	~0.15
3.	Ni-Cr	600	0	NiCr-alloy	<0.1
		800	1.2	NiCr-alloy	~0.1
		1000	2.3	NiCr-alloy, NiO and Cr$_2$O$_3$ (trace)	~0.1
		1200	13.4	NiCr-alloy, NiO and Cr$_2$O$_3$	~0.5
4.	Ni-Cr-Al (alumunizing)	600	0	NiCrAl-alloy	<0.1
		800	1.8	NiCrAl-alloy, α-Al$_2$O$_3$ and Cr$_2$O$_3$ (trace)	<0.1
		1000	2.5	NiCrAl-alloy, α-Al$_2$O$_3$ and Cr$_2$O$_3$ (trace)	~0.1
		1200	14.5	NiCrAl-alloy, α-Al$_2$O$_3$ and Cr$_2$O$_3$	<0.15
* in commensurable quantities					

3.2. Adhesion of Mn-Al washcoat to surface of reticulated foam materials

During exploitation catalysts with washcoated catalytic layer are subjected to the action of high temperatures and gas passing at high flow velocity, causing entrainment of the catalytic coating and a decrease of its catalytic performance. The diffusion layer of α-Al$_2$O$_3$ or Cr$_2$O$_3$ formed on the surface of metal structured materials as a result of aluminization and subsequent treatment in oxidative atmosphere has the role of a buffer sub-layer. Taking into account the equality of the thermal expansion coefficient for majority of oxide phases (8*10^{-6} K^{-1}), the formation of diffusion layer of α-Al$_2$O$_3$ (Cr$_2$O$_3$) allows an increase of adhesion of ceramic coatings to the foam material and prevents detachment and entrainment of the catalytic coating during catalyst exploitation.

The effect of the method of deposition of α-Al$_2$O$_3$ diffusion layer: (1) plasma spray coating [23, 24] and (2) diffusion aluminization [26] on the adhesive strength of alumina layer to the surface of reticulated foam materials based on Ni and Ni-Cr alloy has been studied. In accordance with SEM data, the γ-Al$_2$O$_3$ layer deposited by the suspension method is spread uniformly on the surface of RFM and adjoins it closely (Fig. 3c). The adhesion strength was estimated by the mass loss of the coating during thermocycling based on heating a sample to 900 ºC and fast cooling in water to 25 ºC. The results of thermocycling are shown in Fig. 4.
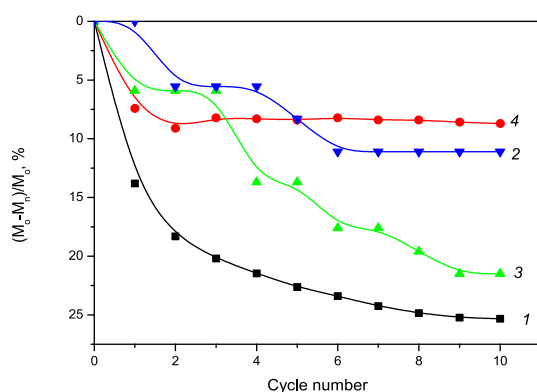

Fig. 4. The mass loss of the washcoating during thermocycling based on heating a sample to 900 ºC and fast cooling in water to 25 ºC. M_o and M_n are mass of washcoating before and after thermocycling, n is a number of thermocycle. (1) NiCr-alloy RFM, (2) NiCr-alloy RFM coated by diffusion layer of α-Al$_2$O$_3$, (3) Ni RFM with diffusion layer of α-Al$_2$O$_3$ supported by diffusion aluminization, and (4) Ni RFM with diffusion layer of α-Al$_2$O$_3$ supported by plasma spray.

From the experimental data it can be seen that the adhesion of the washcoated layer to the surface of RFM depends substantially on the method of formation of diffusion α-Al$_2$O$_3$ layer and chemical composition of the carrier. In case of NiCr materials, the mass loss at thermocycling was 25 and 10 rel.% in case of the absence and the presence of the diffusion α-Al$_2$O$_3$ layer, respectively. The plasma spray deposition of α-Al$_2$O$_3$ provides higher adhesion of

γ-Al$_2$O$_3$ to the surface of the carrier, the mass loss of the washcoated γ-Al$_2$O$_3$ layer at thermocycling did not exceed 8 rel.%. At the same time, the mass loss of the washcoated γ-Al$_2$O$_3$ layer in case of diffusion aluminization attains 22 and 10 rel.% for materials based on Ni and Ni-Cr, respectively. On the other hand, the use of the method of diffusion aluminization provides the formation of diffusion layer of α-Al$_2$O$_3$ across all the article depth, and not only on the article outer surface, as in case of the plasma spraying method. Consequently, the method of diffusion aluminization may appear more promising for the creation of reactors with complex geometry, e.g. reactors in the form of heat exchanging tubes.

3.3. Chemical durability of reticulated foam materials

The data on chemical durability of reticulated foam materials in a solution of nitric acid are given in Table 2. It can be seen that independently on the chemical composition of the framework of the material, the formation of diffusion layer of α-Al$_2$O$_3$ on its surface leads to an increase of its chemical resistance particularly to the 0.5 M solution of nitric acid. It should be noted that the resistance to the dissolution in the nitric acid solution is higher in case of diffusion aluminized material based on Ni in comparison with the material based on Ni-Cr alloy, which is probably due to particular features of the connections in these materials. In the first place, at Ni aluminization the diffusion layer consists of α-Al$_2$O$_3$, while during aluminization of nichrome the surface of the foam material becomes enriched with Cr$_2$O$_3$. Taking into account the fact that the reactivity of Cr$_2$O$_3$ with respect to acids is higher than that of α-Al$_2$O$_3$, the formation of α-Al$_2$O$_3$ prevents the dissolution of the material of the foam framework (Ni and γ-phase) from the volume of the material connections, and consequently helps to preserve the strength characteristics. Secondly, in the process of aluminization of foam materials base on Ni, the formation of nickel aluminides takes place. The formed δ-Ni$_2$Al$_3$ and β-NiAl have high acid resistance and also prevent the extraction of Ni and γ-phase from the material framework.

Table 2
Chemical resistance of reticulated foam materials

#	RFM chemical composition	XRD-phase composition	Properties changes after exposure in 0.5 M solution of HNO$_3$ (25 ºC, 24 h)	
			mass loss, %	shortness (visual)
1.	Ni	Ni^0	7 (Ni is dissolved)	Sample crumbled at mechanical action
2.	Ni-Al - alumunizing	NiAl-alloy, α-Al$_2$O$_3$ and NiO (tr)	3 (Ni and Al are dissolve)	Changes are absented
3.	Ni-Cr	NiCr-alloy	37 (Cr$_2$O$_3$ is dissolved)	Sample crumbled in solution (~25%)
4.	Ni-Cr-Al - alumunizing	NiCrAl-alloy	20 (Cr$_2$O$_3$ is dissolved)	Sample crumbled in solution (~2%)

High chemical stability of structured materials containing diffusion aluminized layer of α-Al$_2$O$_3$ allows deposition of active components, in particular Pt(Pd) and oxides of transition metals (Mn, Fe, Co, Cr, etc.) by the method of capillary impregnation from solution with a low pH value (< 3) without destruction of the carrier and without a decrease of its strength. It should be noted that in most catalytic reactions, catalysts prepared by the method of capillary impregnation (as will be shown below) are active in comparison with catalysts prepared by the suspension method.

Thus, the aluminization of reticulated foam materials based on Ni and Ni-Cr allows both improvement of their operation characteristics (heat durability and heat stability) and an increase of efficiency and life time of the high temperature combustion catalysts prepared on such foam materials. The formation of diffusion aluminized layer of α-Al$_2$O$_3$ allows an increase of adhesion of the catalytic coating to the surface of the foam material, a decrease of the detachment of the coating during temperature drops and a lower entrainment of the active component from the catalyst surface at high velocities of gas flow. In addition, high chemical stability of the material provides possibility of application of capillary impregnation for introduction of active components, thus permitting a reduction in the loss of expensive reagents, such as chloroplatinic and chloropalladic acids and a lower cost of the catalyst production.

3.4 Characterization of the high-temperature manganese-alumina granulated catalyst

For the identification of the most active catalytic compositions, screening of catalytic activity of a series of manganese-alumina catalysts in methane oxidation was performed. Table 3 presents data on the activity of Mn catalysts supported on γ-, ($\gamma+\chi$), and α-Al$_2$O$_3$ aluminas, including a La$_2$O$_3$ – modified sample (5 wt.%).

One can see, the manganese oxides supported on the granulated alumina exhibit a high efficiency in the deep oxidation of hydrocarbons. At first, the XRD-phase composition of alumina does not practically affect the catalyst activity of Mn-catalysts calcined at 900 ºC. The temperature, at which 50% methane conversion is achieved (T$_{50\%}$), constitutes 420-450 ºC for these Mn-catalysts. However, the alumina phase composition significantly affects catalytic activity of the Mn-catalysts calcined at 1100 ºC or 1300 ºC. After catalysts calcination at 1300 ºC, their activity decrease from α-Al$_2$O$_3$ to (γ-+χ)-Al$_2$O$_3$ and to γ-Al$_2$O$_3$. For catalysts annealed at 1100 ºC, the samples on α- and (γ-+χ)-Al$_2$O$_3$ possess the same catalytic activity.

The second, as follows from the Table 3, an increase in the MnO$_x$ concentration from 5 to 10 wt.% provides a slight decrease in the activity of catalyst calcined at 900 ºC. Thus, for the Mn-catalysts based on ($\gamma+\chi$)-Al$_2$O$_3$ and calcined at 900 ºC, T$_{50\%}$ is 400 and 420 ºC, respectively (Samples 3 and 4, Table 3). The similar effect is observed for MnO$_x$ supported on γ-Al$_2$O$_3$ and alumina modified by La$_2$O$_3$. The same trend was found also for catalysts calcined at 1300 ºC. For the α-Al$_2$O$_3$ support, an increase in the manganese loading provides an increase in catalytic activity of the sample after 20 h calcination at 1100 ºC. However, the effect becomes less pronounced on the calcination at 1300 ºC (samples 8 and 9, Table 3).

Table 3
Activity of granulated Mn-Al-O-catalyst calcined at different temperature

#	Support	La loading, wt.% La$_2$O$_3$	Mn loading, wt.% MnO$_2$	T$_{50\%}$, ºC, after calcination at		T$_{50\%}$, ºC, after calcination at 1100 ºC during	
				900 ºC	1300 ºC	4 h	20 h
1.	γ-Al$_2$O$_3$	-	5%	430	620	480	630
2.	γ-Al$_2$O$_3$	-	10%	435	640	-	-
3.	γ- + χ-Al$_2$O$_3$	-	5%	400	540	470	520
4.	γ- + χ-Al$_2$O$_3$	-	10%	420	575	-	-
5.	γ- + χ-Al$_2$O$_3$	5%	5%	430	530	440	470
6.	γ- + χ-Al$_2$O$_3$	5%	10%	420	575	-	-
7[*].	γ- + χ-Al$_2$O$_3$	10%	6%	450	520	430	470
8.	α-Al$_2$O$_3$	-	5%	440	470	470	570
9.	α-Al$_2$O$_3$	-	10%	430	500	440	490
10.	α-Al$_2$O$_3$	5%	5%	450	530	-	480

[*] Sample was prepared by impregnating with a combined solution of Mn and La nitrates, the concentration corresponds to 15% LaMnO$_3$ in the prepared catalyst

Thirdly, as Fig. 5 suggests, the catalysts supported on $(\gamma+\chi)$-Al$_2$O$_3$ and α-Al$_2$O$_3$ modified with La$_2$O$_3$ (Samples 5, 6 and 10, Table 3) exhibit the higher catalytic activity when their calcination proceeds at 1100 ℃. T$_{50\%}$ on these catalysts was 470 and 480 ℃, respectively. The γ-Al$_2$O$_3$ supported catalyst shows low thermal stability.
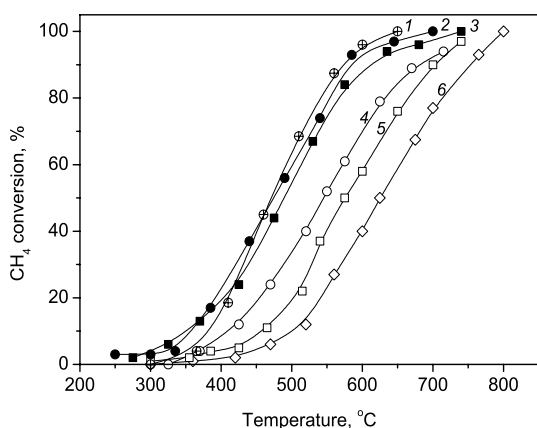

Fig. 5. Methane conversion in CH$_4$ oxidation on catalysts calcined at 1100 ℃/20 h: (1) – 15% LaMnO$_3$/5%-La$_2$O$_3$/$(\gamma+\chi)$-Al$_2$O$_3$; (2) – 5% MnO$_2$/5%La$_2$O$_3$/$(\gamma+\chi)$-Al$_2$O$_3$, (3) –5% MnO$_2$/5%La$_2$O$_3$/α-Al$_2$O$_3$; (4) – 5% MnO$_2$/$(\gamma+\chi)$-Al$_2$O$_3$, (5) – 5% MnO$_2$/α-Al$_2$O$_3$ and (6) – 5% MnO$_2$/γ-Al$_2$O$_3$.

Fourthly, the curves of methane conversion of the catalysts supported on La$_2$O$_3$-modified $(\gamma+\chi)$-Al$_2$O$_3$ versus thermal treatment conditions are shown in Fig. 6. The figure shows that after high-temperature treatment at 1100 ℃, the above catalyst provides 90-98% conversion of methane at 650 ℃, though their activity decreased with calcination temperature (1300 ℃).
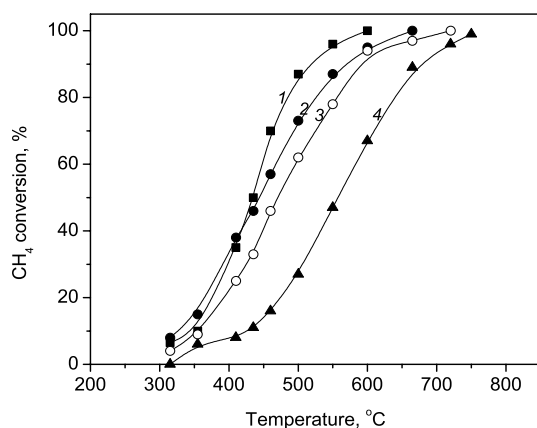

Fig. 6. Methane conversion in CH$_4$ oxidation on 5% MnO$_2$/5%La$_2$O$_3$/$(\gamma+\chi)$-Al$_2$O$_3$ calcined at 900 ℃/4 h (1), 1100 ℃/4 h (2), 1100 ℃/20 h (3) and 1300 ℃/4 h (4).

Fifthly, the catalyst prepared by impregnation of La$_2$O$_3$-modified alumina with a joint solution of Mn and La nitrate (atomic ratio Mn/La = 1) possessed a high catalytic activity (Sample 7, Table 3).

Phase composition was studied to find a correlation between Mn-containing phase and catalytic activity. For catalyst on unmodified supports γ- and $(\gamma+\chi)$-Al$_2$O$_3$ calcined at 500 ℃, we observed the formation of coarse-dispersed crystallized phases MnO$_2$ and β-Mn$_2$O$_3$ with coherent-scattering region about 200 Å (Table 4). As the concentration of manganese increases, a spinel-type solid solution (Mn,Al)[Al]$_2$O$_4$ forms, the lattice parameter is ~8.115 Å (Samples 2 and 4, Table 4). As the calcination temperature is increased to 900 ℃ and then to 1100 and 1300 ℃, the improvement of solid solutions is observed. Finally, phase α-Al$_2$O$_3$ and a number of spinels from (Al,Mn)[Al]$_2$O$_4$ to partially converted spinels (Mn,Al)[Mn,Al]$_2$O$_4$ are formed.

High catalytic activity and thermal stability of the La$_2$O$_3$-modified Mn-Al-O catalysts can be explained by formation of solid solutions based on γ-Al$_2$O$_3$ structure at 500-900 ℃ due to the interaction between a manganese oxide and alumina [20, 22]. At 900 ℃ the interaction is more pronounced. It results in the formation of a number of solid solutions Mn-La-γ*-Al$_2$O$_3$ based on spinel structure of γ-Al$_2$O$_3$, the crystallized manganese phases are not observed (Samples 5 and 6, Table 4). The solid solutions Mn-La-γ*-Al$_2$O$_3$ are precursors of hexaaluminates MnLaAl$_{11}$O$_{19}$ formed at 1300 ℃. By analogy with the regularities observed in the Mg-La-Al-O-system [33], the excess of manganese (not included in the hexaaluminates composition) forms a manganese-alumina spinel during the solid solution decomposition at high-temperature calcination (Samples 6, Table 4).

For the α-Al$_2$O$_3$-based catalysts (Sample 9, Table 4), an increase in the calcination temperature from 900 ℃ to 1300 ℃ results in the formation of two phases of spinel-based solid solution with the lattice parameter ~8.056 Å and ~8.135 Å. Thus, one may suggest that high activity and thermal stability of the α-Al$_2$O$_3$-based catalysts is provided by the formation of a structure, which is close to the structure of spinel. In [23], the activation of Mn$_2$O$_3$/α-Al$_2$O$_3$ system upon the calcination at 900-1000 ℃ is explained by the formation of the highly dispersed phase with an approximate composition Mn$_3$O$_{4,2}$ and the defect structure of spinel.

The high catalytic activity of sample prepared by impregnation of La$_2$O$_3$-modified alumina with a joint solution of Mn and La nitrate (Sample 7, Table 4) is explained by formation of La$_{1-x}$Mn$_x$O$_3$.

Table 4
Phase composition of granulated Mn-Al-O catalysts as function of chemical composition and calcination temperature

#	Support	La$_2$O$_3$, wt.%	MnO$_2$, wt.%	Phase composition at calcination temperature		
				500 ºC	900 ºC	1300 ºC
1.	γ-Al$_2$O$_3$	-	5	MnO$_2$ γ*-Al$_2$O$_3$ (a~7.910A)	γ*-Al$_2$O$_3$ δ-Al$_2$O$_3$ α-Al$_2$O$_3$	(Mn$_1$Al)[Al]$_2$O$_4$ (a~8.125A) (Mn$_1$Al)[Mn$_1$Al]$_2$O$_4$ (a~8.290A) α-Al$_2$O$_3$
2.	γ-Al$_2$O$_3$	-	10	MnO$_2$ β-Mn$_2$O$_3$ γ*-Al$_2$O$_3$ (a~7.910A) *** (a~8.115A)	γ-Mn$_3$O$_4$, trace γ*-Al$_2$O$_3$ θ-Al$_2$O$_3$ α-Al$_2$O$_3$	(Mn$_1$Al)[Mn$_1$Al]$_2$O$_4$ (a~8.285A) α-Al$_2$O$_3$
3.	γ- + χ-Al$_2$O$_3$	-	5	MnO$_2$ γ-Al$_2$O$_3$ (a~7.910A)	β-Mn$_2$O$_3$ (trace) γ*-Al$_2$O$_3$ δ*-Al$_2$O$_3$ α-Al$_2$O$_3$	(Mn$_1$Al)[Al]$_2$O$_4$ (a~8.097A) (Mn$_1$Al)[Mn$_1$Al]$_2$O$_4$ (a~8.285A) α-Al$_2$O$_3$
4.	γ- + χ-Al$_2$O$_3$	-	10	MnO$_2$ β-Mn$_2$O$_3$ γ-Al$_2$O$_3$ (a~7.905A) *** (a~8.115A)	γ-Mn$_3$O$_4$ γ*-Al$_2$O$_3$ (a~7.92-8.17A) θ-Al$_2$O$_3$ α-Al$_2$O$_3$	(Mn$_1$Al)[Al]$_2$O$_4$ (a~8.078A) (Mn$_1$Al)[Mn$_1$Al]$_2$O$_4$ (a~8.270A) α-Al$_2$O$_3$
5.	γ- + χ-Al$_2$O$_3$	5	5	γ*-Al$_2$O$_3$ (a~7.952A)	γ* Al$_2$O$_3$ (a~7.970A)	MnAl$_{11}$LaO$_{19}$ α-Al$_2$O$_3$
6.	γ- + χ-Al$_2$O$_3$	5	10	β-Mn$_2$O$_3$ γ*-Al$_2$O$_3$ (a~7.910A)	γ*-Al$_2$O$_3$ (a~7.931A)	(Mn$_1$Al)[Mn$_1$Al]$_2$O$_4$ (a~8.280A) MnAl$_{11}$LaO$_{19}$ α-Al$_2$O$_3$
7.	γ- + χ-Al$_2$O$_3$	10	6	γ*-Al$_2$O$_3$	Mn$_2$O$_3$ La$_{1-x}$Mn$_x$O$_3$ δ-Al$_2$O$_3$	MnLaAl$_{11}$O$_{19}$ α-Al$_2$O$_3$
9.	α-Al$_2$O$_3$	-	10	-	Mn$_3$O$_4$ (a~8.056A) ***(a~8.135A) α-Al$_2$O$_3$	Mn$_3$O$_4$ (a~8.056A), trace ***(a~8.147A) α-Al$_2$O$_3$

γ*- Al$_2$O$_3$ – solid solution Mn-La-γ*-Al$_2$O$_3$ based on the structure of Al$_2$O$_3$; *** – solid solution based on spinel structure MnAl$_2$O$_4$ similar to (Mn,Al)[Al]$_2$O$_4$; where (Mn,Al) – tetrahedral, [Al] – octahedral lattice positions

3.5. Manganese-alumina washcoated on highly porous reticulated foam materials

The manganese was introduced on the surface of ceramic and Ni-Cr-alloy foam either by wet impregnation of alumina-washcoat (Method 1) or by dip coating into the Mn-alumina containing suspension (Method 2) with subsequent high-temperature activation at 900 ºC, as described in [20]. Data on the activity of RFM-based washcoated catalysts in the methane oxidation with respect to compositions of the washcoat (alumina phase compositions, modified additives and manganese oxide loading) are given in Tables 5 and 6. Tables 5 and 6 show that the catalysts prepared by method 1 are more active than those prepared by method 2 (Samples 3, Tables 5 and 6), T$_{50\%}$ is 470 and 525 ºC, respectively.

The catalytic activity of the washcoated monoliths in the methane combustion has been compared with those of Mn-aluminas powders. The regularities observed for granulated Mn-Al-O catalysts, such as the influence of alumina phase composition, Mn loading and modified additivies on catalytic activity, were also typical of the RFM-supported catalysts. For examples, when the manganese loading in the washcoat increases from 5 to 10 wt.%, the activity of the catalysts with the (γ+χ)-Al$_2$O$_3$ washcoat (T$_{50\%}$ = 480-490 ºC) does not change. By contrast, the activity of the catalysts with an α-Al$_2$O$_3$ washcoat decreases significantly with Mn-loading, T$_{50\%}$ = 500 and 560 ºC, respectively. Modifying of the alumina-washcoat with lanthanum oxide (5 wt.%) results in a small increase of the catalyst activity.

For the catalysts prepared by Method 2, the effect of phase composition of the alumina support, manganese concentration and presence of a modifier becomes less pronounced. When the concentration of the washcoat is ~ 15 wt.%, T$_{50\%}$ is 520-530 ºC. For the catalysts with α-Al$_2$O$_3$ washcoat, T$_{50\%}$ was 550 ºC. The increase of the washcoat loading to ~ 20 wt.%

leads to higher catalytic activity, $T_{50\%}$ is 500-505 ºC.

Thermal stability of the washcoated catalysts based on RFM-NiCr with different compositions of the washcoat was studied during their treatment in the flow of 9 vol.% CH_4 with air at 1100 ºC and at space velocity 10000 h^{-1} for 50 h. Data on the catalytic activity are given in Fig. 7. One can see, the $T_{50\%}$ for the La_2O_3-modified Mn-alumina sample (Curve 2, Fig. 7) decreases steadily from 550 to 725 ºC during 50 h of treatment. For the unmodified sample, the similar activity decrease was observed during 10 h of treatment (Curve 1, Fig. 7). The sample prepared by impregnation of La_2O_3-modified alumina with a joint solution of Mn and La nitrate (Sample 7, Table 4) and contained $La_{1-x}Mn_xO_3$ active phase characterized by the better thermal stability. Its $T_{50\%}$ change from 525 to 600 ºC for 50 h of testing (Fig. 7, Curve 3).

So, the deposition of the La_2O_3-modified Mn-alumina and $Mn_xLa_{1-x}O_3$ catalyst on the surface of RFM allows one to obtain new more thermally stable and efficient catalysts. These catalysts significantly outperform the known Pt/Al_2O_3 and $LaCoO_3/Al_2O_3$ catalysts deposited in the same way on RFM on methane oxidation activity (Fig. 8) and thermal stability. Mixed oxides with a perovskite structure ($LaMO_3$, where M is Co, Mn, Fe) are the most active catalysts in the reaction of high-temperature hydrocarbon ox-

idation. However, the activity of $LaCoO_3$ catalysts supported on RFM with a washcoating based on γ-Al_2O_3 with and without a modifying additive La_2O_3, decreased after long (more than 15 h) calcination at 1000 ºC [24]. The catalytic section of the water-heating boiler is filled with the La_2O_3-modified manganese-aluminum oxide catalyst supported on the surface of highly porous reticulated foam materials.
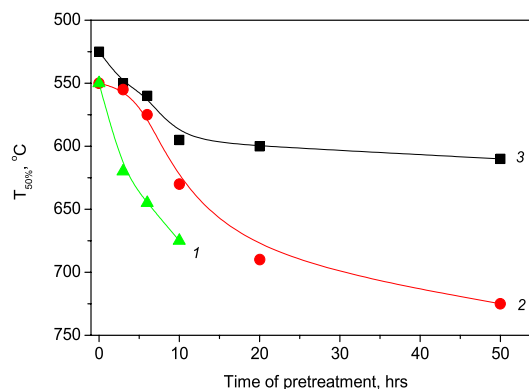

Fig.7. Temperature of 50% of methane conversion over Mn-Al-O catalysts washcoated on RFM versus time of pretreatment in mixture (9 vol.% CH_4 with air) at 1100 ºC and 10000 h^{-1}: 1 – 10%MnO_2/γ-Al_2O_3/RFM (Sample 1, Table 6); 2 – 5%MnO_2/5%La_2O_3/γ-+χ-Al_2O_3/RFM (Sample 2, Table 6); 3 – 15%$LaMnO_3$/2.5%La_2O_3/γ-+χ-Al_2O_3/RFM (Sample 7, Table 6).

Table 5

Activity of Washcoated Catalysts Based on RFM prepared by Method 1. Support: RFM – NiCr. Washcoat loading was 15 wt.%

#	Washcoated Catalyst Composition			$T_{50\%}$, ºC, after calcination at 900 ºC
	Alumina composition	La loading in washcoat, wt.% La_2O_3	Mn loading in washcoat, wt.% MnO_2	
1.	γ- +χ-Al_2O_3	-	5.0	490
2.	γ- +χ-Al_2O_3	-	10.0	480
3.	γ- +χ-Al_2O_3	5.0	5.0	470
4.	α-Al_2O_3	-.	5.0	500
5.	α-Al_2O_3	-	10.0	560
6.	α-Al_2O_3	5.0	5.0	500

Table 6

Activity of Washcoated Catalyst based on RFM prepared by Method 2. Support: RFM – NiCr

#	Washcoated Catalyst composition					$T_{50\%}$, ºC, after calcination at 900 ºC
	Washcoat loading, wt%.	Mn-Catalyst in washcoat		La loading in washcoat, wt.% La_2O_3	Mn loading in washcoat, wt.% MnO_2	
		No samples from Table 3	Alumina support			
1.	15	No. 2	γ-Al_2O_3	-	7.8	550
2.	15	No. 5	γ+χ-Al_2O_3	4.2	4.2	525
3.	15	No. 8	α-Al_2O_3	-	4.0	530
4.	20	No. 3	γ+χ-Al_2O_3	-	4.3	505
5.	20	No. 5	γ+χ-Al_2O_3	4.2	4.2	500
6.	20	No. 9	α-Al_2O_3	-.	7.6	500
7.	20	No. 7	γ+χ-Al_2O_3	8.5	5.6	500

Table 7
Physicochemical properties and external size of RFM used for preparation
of the pilot catalytic heat-exchanger and catalytic burner

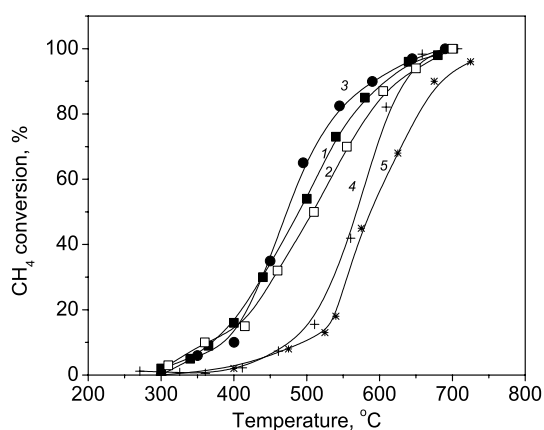| #	Support	Physicochemical properties				External size, cm
		Average size of cell, mm/wall thickness, mm/density, g/cm³	S_{sp}, m²/g	Pore volume, cm³/g	XRD	
1.	RFM-Ni-Cr	2-3 / 0.2-0.3 / 0.50	0.2	0.	Ni-Cr-alloy	25 × 25
2.	RFM-ceramics	2-3 / 0.3-0.5 / 0.33	1.5	0.1	$\alpha - Al_2O_3$ (70-80%) cordierite (20-30%) $\alpha - SiO_2$ (trace)	diameter 25

Fig 8. Activity of Mn catalysts supported on $(\gamma+\chi)$-Al$_2$O$_3$ washcoated Ni-Cr foam material and calcined at 900 ºC. 5% MnO$_2$ supported by wetness impregnation (1) and dip coating (2), 5% MnO$_2$ supported by wetness impregnation over La$_2$O$_3$-modified alumina (3). For comparison are presented: 0.46% Pt /γ-Al$_2$O$_3$ (T$_{calc.}$ = 800 ºC, method 2, (4) and 15% La-Co-O/γ-Al$_2$O$_3$ (T$_{calc.}$ = 800 ºC, method 1, (5)).

3.6. Application of the high-temperature Mn-La-Al-O catalysts in a catalytic heat-exchanger

The developed high-temperature Mn-La-Al-O catalyst has been tested in a catalytic combustion chamber intended for flameless fuel combustion. Physicochemical properties and external size of RFM used for preparation of the pilot catalytic burner are given in Table 7.

The first type of the heat-exchanger was designed in the form of a number of tubes situated in the highly porous reticulated foam matrix of the Ni-Cr alloy (Fig. 9a). The principle of making the catalytic heat-exchanger consists of duplicating the structure of open-cellular polyurethane foam over metal tubes using the suspension-electrochemical method. Then the thermal destruction of the organic component carries out for formation of NiCr-alloy. The conditions of powder deposition, chemical and electrolytic coatings on the metal-polymeric mod-

el as well as the conditions of subsequent low- and high-temperature treatment were optimized to provide low thermal resistance between the heat-exchanging highly porous RFM and the metal tubes [25]. The catalytic washcoat based on the Mn-La-Al oxides composition was deposited on surface of RFM by using the dip coating. It was treated next at 900 ºC in air in order to transfer pseudoboehmite binder to alumina.
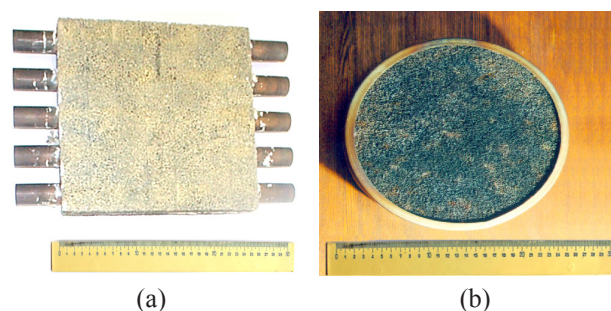

(a)   (b)

Fig. 9. External view of the catalytic heat-exchanger (NiCr-alloy RFM washcoated by Mn-La-Al catalyst, (a) and the catalytic block in water-heating boiler (Cordierite RFM washcoated by Mn-La-Al catalyst, (b).

The second type of the catalytic burner comprises two ceramic foam plates with the different pore parameters, placed in a drum and sealed over the perimeter by thermostable mineral insulation (Fig. 9b). The upper RFM plate with the deposited catalytic Mn-La-Al-coating acts as a catalytic reactor, in which the methane deep oxidation takes place. The function of the lower foam plate is to prevent the ignition of the fuel-air mixture in the mixing chamber.

The second catalytic burner was tested as part of the water-heating boiler prototype. The catalytic water-heating boiler prototype was a welded apparatus containing a cylindrical water-filled tank with a mineral thermal insulation and 'fire-tubes' vertical placed into the tank. Below the water-filled tank were situated the catalytic burner and a fuel-air pre-mixing chamber. The boiler load-carrying structure

combines the water-filled tank, the catalytic burner, the igniter, the automatic control and safety devices, and a flue gas collector into a single construction covered by removable metal sheets.

Natural gas was introduced through automatic control and safety device into the nozzles of injectors of fuel-air mixing chamber. Air is drawn through the injectors due to the energy of gas jet and the underpressure formed. The prepared air-fuel mixture is fed to the catalytic block. The heat energy of the hot ceramic foam plate was used for thermal radiation, which is absorbed by water through a furnace wall, and for warming-up of the incoming fuel-air mixture. The heat energy of combustion products was used for the water heating through the walls of convective heat exchanger and, partly, through the furnace wall. After the heating of catalyst, the furnace acted only as the heat-absorbing surface. The starting of boiler was accomplished by means of the ignition torch of 200 W power equipped with the control thermocouple and piezoelectric spark plug.

The combustion products passed from the furnace into the convective heat exchanger, consisting of the tubes with turbulators, which increased the heat-transfer coefficient from combustion products to water. The combustion products cooled below 150 ºC were directed into the flue gas collector and further into the flue. The water circulation was supporting natural convection.

The technical characteristics of the catalytic boiler prototype were as follows:

Heat power – 16 kW
Fuel – natural gas (the pressure is 130 mm water column)
Heat efficiency – ≥88-94%
Pressure of circulating water – 0.065 MPa
Water temperature – 50-90 ºC
Dimensions – 890×440×440 mm
Weight – 90 kg.

Testing of the catalytic boiler prototype upon the variation of different regime parameters (air excess coefficient, heat power, etc.) was carried out. The testing results presented in Table 6 show that practically total oxidation of natural gas occurs in the boiler over the range of heat power 8.3-16.1 kW with the air excess coefficient α = 1.4-2.3 and the catalyst temperature 700-800 ºC. As can be seen from the Table 8, the concentrations of toxic compounds in flue gas calculated for a stoichiometric gas mixture (α = 1) are very low: 2-8 ppm of nitrogen oxides and 0-60 ppm of carbon monoxide. Note that toxic component concentration were significantly lower compared with the conventional household boilers.

Table 8
Testing data of a prototype catalytic water-heating boiler

Heat power, kW	Heat efficiency, %	Air excess coefficient (α)	Concentrations of toxic compounds in flue gas calculated for α=1, ppm			Catalyst temperature, ºC
			CO	NO$_x$	SO$_2$	
16.1	85.4	2.2	59.4	4.4	0	800-850
16.1	88.5	1.8	53.4	5.3	0	800-850
15.0	90.9	1.4	0	7.0	2.8	830-870
13.8	90.9	1.6	14.0	7.8	3.1	830-870
12.7	91.8	1.6	0	7.8	3.1	860-880
12.6	91.6	1.6	1.6	6.2	0	880-920
12.5	89.3	1.7	0	3.4	0	850-860
12.5	92.0	1.6	1.6	6.4	0	530-860
12.5	92.0	1.4	1.4	5.8	0	530-860
11.1	88.4	2.0	0	4.1	0	750-850
11.1	87.4	2.3	46.0	2.3	2.3	750-850
8.3	94.0	2.0	0	4.0	0	750-800

3.7. Characterization of the spent catalyst

During running in the catalytic heat-exchanger and water-heater the catalyst undergoes local overheating, which can causes the catalyst deactivation due to change of its composition and surface area. Therefore after testing of the catalytic water-heating boiler prototype, the spent catalyst has been characterized in order to have an insight into the deactivation process. The changes taking place are observed even by sight following the variation of catalyst color: from deep-brown (initial) to black in the lower part and pink in the upper part of catalytic block. The nitrogen adsorption technique shows that the spent catalyst undergoes sintering with reduction of the surface area from 26 m^2/g (which characterizes the initial catalyst calcined at 500 ºC) to 10 m^2/g in the lower part and 3 m^2/g in the upper part. Note that the surface area of the catalyst calcined at 900 ºC during 4 h was 13 m^2/g.

The diffraction patterns of the Mn-La-Al-O-catalyst supported on cordierite-based RFM and calcined at 500-900 ºC are completely identical to one of the RFM. The XRD analysis of the spent catalyst fragments, which were cut from different part of spent catalytic block, visually differing by color, shows that the new phases are appearing. These phases are characterized by the single maximum at 2θ = 31.8º for the fragment from the upper part and at 2θ = 33.3º for the fragment from the lower part, that makes difficult their XRD identification.

Catalytic activity of Mn-La-Al-O-catalyst fragments, which were cut from the upper and lower parts of the catalytic block, in the methane oxidation

is presented in Fig. 10. For comparison, the activity of the initial Mn-LaAl-O-catalysts calcined at 500 and 900 ºC is also shown on Fig. 10. Figure 10 shows that the catalyst indeed undergoes deactivation during running in water-heating prototype. For example, $T_{50\%}$ is 450 ºC for the initial catalyst, 520 ºC for the fragment from the lower part of catalytic block and 620 ºC for the fragment from its upper part. We believe that a modifying of the Mn-La-Al-O-catalyst with additive of other rare-earth metal oxides (La-Mg or Ce-Mg) allow a increasing of thermal stability to 1100-1300 ºC [19, 20] and, consequently, extends the temperature range of catalyst operation.

4. Conclusion

The deposition of a La_2O_3-modified Mn-Al-O catalyst on the surface of RFM allows us to obtain new more thermally stable and efficient catalysts. These catalysts outperform the known Pt/Al_2O_3 and $LaCoO_3/Al_2O_3$ catalysts supported by the same way on RFM surface. They exhibit higher thermal stability.

Testing of the catalytic water-heating prototype consisting of the La_2O_3-modified Mn-Al-O catalyst on RFM shows a considerable reduction in the emissions of NO_x and CO compared to the conventional household boilers. Its using provides a decrease in the gas consumption and prevents evolution of harmful emissions to the atmosphere.

The employment of the NiCr and ceramic highly porous reticulated foam materials in catalytic combustion chamber provides a high specific heat productivity and good heat transfer, thus reducing the dimensions and the weight of the boiler.
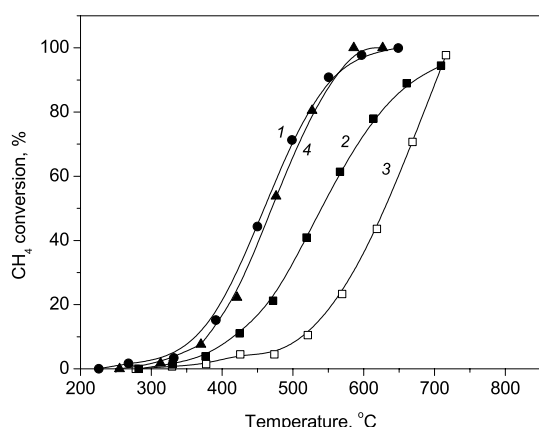

Fig 10. Activity of MnO_x on La_2O_3 – modified γ-Al_2O_3 composition washcoating over RFM-cordierite and calcined at 500 ºC: the initial (1) and after operation in a catalytic water-heating boiler – the fragment from the lower part (2) and the fragment from the upper part (3) of catalytic block. For comparison the activity of this catalyst calcined at 900 ºC (4) is presented.

References

[1]. G.K. Boreskov, E.A. Levitskii, Z.R. Ismagilov, Zh. Vsesoyuznogo Khimicheskogo Obshchestva im. D.I.Mendeleeva 29: 379 (1984)
[2]. Z.R. Ismagilov, M.A. Kerzhentsev, Catal. Today 47 (1999) 339–346.
[3]. Z.R. Ismagilov, M.A. Kerzhentsev, S.A. Yashnik, N.V. Shikina, A.N. Zagoruiko, V.N. Parmon, V.M. Zakharov, B.I. Braynin, O.N. Favorski, Development of Granular Catalysts and Natural Gas Combustion Technology for Small Gas Turbine Power Plants. In book "Gas Turbines", Ed.: I. Gurrapa, Sciyo, Chapter 4: 79 (2010). ISBN 978-953-307-146-6.
[4]. S.A. Yashnik, V.V. Kuznetsov, Z.R. Ismagilov, V.V. Ushakov, N.M. Danchenko, S.P. Denisov Topics in Catal. 30/31 (2004) 293–298.
[5]. S.A. Yashnik, Z.R. Ismagilov, A.V. Porsin, S.P. Denisov, N.M. Danchenko, Topics in Catal. 465 (2007) 42–43.
[6]. R.M. Heck, R.J. Farrauto, Catalytic air pollution control. Commercial Technology. New York, VNR, 1995, P.206.
[7]. M.V. Twigg Catal. Today 117 (2006) 407–418.
[8]. R.A. Dalla Betta, Catal. Today 35 (1997) 129–135.
[9]. J.G. McCarty, M. Gusman, D.M. Lowe, D.L. Hildebrand, K.L. Lau, Catal. Today 47 (1999) 5–17.
[10]. R.J. Farrauto, M.C. Hobson, T. Kennelly, E.M. Waterman, Appl. Catal. A 81 (1992) 227–237.
[11]. H. Arai, T. Yamada, K. Eguchi, T. Seiyama, Appl. Catal. 26 (1986) 265–276.
[12]. G. Saracco, F. Geobaldo, G. Baldi, Appl. Catal. B: Environ. 20 (1999) 277–288.
[13]. M. Machida, K. Eguchi, H. Arai, J. Catal. 103 (1987) 385–393.
[14]. M. Machida, K. Eguchi, H. Arai, J. Catal. 120 (1989) 377–386.
[15]. M. Machida, K. Eguchi, H. Arai, Chem. Lett. 767–770 (1987).
[16]. S.A. Yashnik, Z.R. Ismagilov, V.V. Kuznetsov, V.V. Ushakov, V.A. Rogov, I.A. Ovsyannikova, Catal. Today 117 (2006) 525–535.
[17]. F. Laville, D. Gourier, A.M. Lejus, D. Vivien, J. Solid. State Chem. 49 (1983) 180–187.
[18]. Z. Jaworska-Golas, W. Mista, J. Wrzyszcz, Catal. Lett. 24 (1994) 133–139.
[19]. L.T. Tsykoza, Z.R. Ismagilov, V.V. Ushakov, V.V. Kuznetsov, I.A. Ovsyannikova, Kinet. Katal. 44: 879 (2003).

[20]. Russian Application 2185238 (2002) L.T. Tsykoza, S.A. Yashnik, Z.R. Ismagilov. Catalyst for high-temperature combustion of hydrocarbon fuels.

[21]. S.A. Yashnik, Z.R. Ismagilov, Topic Catal. 55 (2012) 818–836.

[22]. P.G. Tsyrulnikov, V.S. Salnikov, V.A. Drozdov, S.A. Stuken, A.V. Bubnov, E.I. Grigorov, A.V. Kalinkin, V.I. Zaikovskii, Kinetics and Catalysis 32 (1191) 439–441.

[23]. Z.R. Ismagilov, V.V. Pushkarev, O.Yu. Podyacheva, N.A. Koryabkina, H. Veringa, Chem. Eng. J. 82 (2001) 355–360.

[24]. O.Yu. Podyacheva, N.V. Shikina, Z.R. Ismagilov, V.A. Ushakov, A.I. Boronin, N.A. Rudina, I.A. Ovsyannikova, S.A. Yashnik, O.P. Solonenko, A.A. Michal'chenko, H. Veringa, Chemistry for Sustainable Development 11 (2003) 233–238.

[25]. V.N. Antsiferov, O.P. Kocheev, A.P. Kunevich, Patent 1640208. The method of galvanoplastic manufacture of the reticulated foam material. Public. 07.04.91 (in Russian).

[26]. A. Leonov, A. Romashko. In book "Cellular Metals and Metal Foaming Technology", 3rd Int. Seminar «MetFoam 2003» / Ed.: J. Banhart, N. Fleck, Berlin: Verl. MIT Publ. 62 (2003).

[27]. J.S. Church, N.W. Cant, D.L. Trimm, Appl. Catal. A 101 (1993) 105–116.

[28]. R.A. Shkrabina, N.A. Koryabkina, V.A. Ushakov, E.M. Moroz, Z.R. Ismagilov, M. Lausberg, Kinetics and Catalysis 37 (1996) 109–116.

[29]. X-ray Powder Diffraction File JCPDS-ICDD.

[30]. V.V. Ushakov, R.A. Shkrabina, N.A. Koryabkina, Z.R. Ismagilov, Kinetics and Catalysis 38 (1997) 117–123 .